Journal of Chromatography A, 1549 (2018) 63–76

Contents lists available at ScienceDirect

Journal of Chromatography A

journal homepage: www.elsevier.com/locate/chroma

Utility of a high coverage phenyl-bonding and wide-pore superficially porous particle for the analysis of monoclonal antibodies and related products

Balázs Bobály[a], Matthew Lauber[b], Alain Beck[c], Davy Guillarme[a], Szabolcs Fekete[a,*]

[a] School of Pharmaceutical Sciences, University of Geneva, University of Lausanne, Bd d'Yvoy 20, 1211 Geneva 4, Switzerland
[b] Waters Corporation, 34 Maple Street, Milford, MA 01757-3696, United States
[c] Centre d'Immunologie Pierre Fabre, 5 Avenue Napoléon III, 74160 Saint-Julien-en-Genevois, France

ARTICLE INFO

Article history:
Received 11 December 2017
Received in revised form 13 February 2018
Accepted 21 March 2018
Available online 21 March 2018

Keywords:
Superficially porous
Wide-pore
Phenyl bonding
Column efficiency
Monoclonal antibody
Antibody-drug-conjugate

ABSTRACT

A wide-pore silica-based superficially porous material with a high coverage phenyl bonding was evaluated for the analysis of monoclonal antibodies and antibody-drug conjugates. This new material is based on 2.7 μm particles having a shell thickness of 0.40 μm and average pore size of approximately 450 Å.

Various important features of this reversed phase column technology were explored, including kinetic performance for large biomolecules (i.e. speed of analysis, efficiency and peak capacity), recovery of proteins, selectivity for resolving modifications, and the possibility to reduce the amount of trifluoroacetic acid in the mobile phase. A systematic comparison was also performed with other existing modern wide-pore phases possessing differences in structure/morphology and chemistry.

If all these figures of merit are considered, it is clear that this phenyl bonded wide-pore superficially porous stationary phase is one of the most promising materials to have been developed in recent years. Indeed, it offers kinetic performance comparable to the most efficient wide-pore SPP column on the market. In terms of protein recovery, this new phase was found to be superior to silica-based and silica-hybrid C4 bonded materials, particularly with separations performed at sub-80 °C temperature. Under such conditions, it in fact shows recoveries that are quite similar to a divinyl benzene (DVB) polymer-based material. More importantly, due to its unique, high coverage phenyl bonding, it offers additional steric effects and potentially even π-π interactions that yield advantageous selectivity for mAb subunit peaks and ADC species as compared to commonly used C4 or C18 bonded phases. Last but not least, mobile phases consisting of only 0.02–0.05% trifluoroacetic acid can be successfully used with this column, without significant loss in recovery and peak capacity.

1. Introduction

During the last decade, there have been several innovations in column technology and instrumentation to improve the separation power in reversed-phase liquid chromatography (RPLC) of proteins. The aim of these developments has been to achieve higher efficiency and faster analysis for large molecules that possess slow diffusivity and tend to adsorb strongly and heterogeneously to stationary phases and system surfaces (tubing, injector).

Superficially porous particle (SPP) structure is still one of the most advantageous stationary phase morphologies for macromolecule separations, as the solute diffusion distance inside the particles plays probably the most important role in the mass transfer process for slowly diffusing solutes [1–8]. The capability of columns packed with SPPs, manifest as unusually high efficiency at modest operating pressure, quickly resulted in the commercial introduction and success of products branded as being based on so-called porous shell, core–shell or fused-core particles [9–11]. Indeed, the efficiency of columns packed with SPPs increases as the porous shell thickness decreases. However, the optimum shell thickness in reality is a compromise between efficiency, sample loading capacity and analyte retention [12]. It appears that the structure of the latest generation of SPPs is very close to the optimum and a balance between column efficiency and loadability. A 160 Å 2.7 μm packing with a shell thickness of 0.5 μm was introduced in 2010 under the brand names of HALO Peptide ES-C18 and Ascentis Express Peptide ES-C18, respectively [13,14]. An average pore size of ~160 Å allowed the unrestricted access of molecules

* Corresponding author.
E-mail addresses: szabolcs.fekete@unige.ch, szfekete@mail.bme.hu (S. Fekete).

https://doi.org/10.1016/j.chroma.2018.03.043
0021-9673/

up to approximately 15 kDa, depending on their molecular conformation [15]. Kirkland et al. systematically compared the efficiency of the 160 Å HALO Peptide ES-C18 column to the original 90 Å HALO-C18 column for mixtures of peptides and small proteins [14]. In 2012, a larger (3.6 μm) SPP wide-pore material (0.2 μm shell thickness) was launched under the name of Aeris Widepore, and seemed to be very promising for large protein separations including monoclonal antibody (mAb) fragments [16,17]. Its relatively large particle diameter afforded low column pressures, which help to minimize on-column degradation of pressure sensitive proteins by way of avoiding high shear forces and to minimize pressure induced increases in hydrophobic retention that can broaden peaks. To analyse intact large proteins and their sub-units, the particle size and shell thickness were further optimized [18]. Theory and previous studies indicated that a thin shell should be used to compensate for the low diffusion coefficients and resulting poor mass transfer of large molecules. To find the optimum, three different batches of 3.4 μm particles with 400 Å pores were compared with 0.15, 0.20 or 0.25 μm-thick shells (these particles had surface areas of 10, 15 and 18 m^2/g) in an experimental study [18]. It was found that a 0.20 μm thick shell (400 Å) provided the most preferred chromatographic performance for proteins. This material is now commercially available under the brand name of HALO Protein.

Recently a one-step coating coacervation method was developed for the synthesis of a series of wide pore SPPs of different particle sizes, pore sizes, and shell thicknesses [1]. The effects of pore size (300 Å vs. 450 Å), shell thickness (0.25 μm vs. 0.50 μm), and particle size (2.7 μm and 3.5 μm) on the separation of large proteins, intact and fragmented mAbs were systematically studied with this recent one-step coating method. It was found that the larger pore size actually had more impact on the kinetic performance achieved with mAbs, than the particle size and shell thickness. The SPPs with larger 3.5 μm particle size and larger (450 Å) pore size showed the highest resolution for mAbs [1]. The results led to the optimal particle design with a particle size of 3.5 μm, a thin shell of 0.25 μm and pore size of 450 Å. This material is now commercialized as AdvanceBio RP-mAb.

SPPs with 1000 Å pores designed specifically for separating large biomolecules and industrial polymers have been described [19]. Separations of large biomolecules confirmed the advantages of particles with very large pores in minimizing mass transport effects for improved resolution. Studies with known DNA fragments indicated that the 1000 Å particles separate 1000 base pairs DNA (approximately 660 kDa) with minimal effects of restricted diffusion [19].

The so called sphere-on-sphere (SOS) particle structure is quite close to SPP morphology. This approach provides a simple and fast one-pot synthesis in which the thickness, porosity and chemical substituents of the shell can be controlled by using the appropriate reagents and conditions [20]. These SOS columns were found to be particularly well suited for the analysis of large biomolecules, since each particle is composed of a relatively large solid inner core surrounded by a significant number of small spheres of silica [21]. Thanks to the special particle morphology, the surface area seems to be sufficient to achieve reasonable loading capacity and retention. This prototype SOS material was successfully applied for the separation of model proteins, mAbs and antibody-drug conjugate (ADC) [21].

By using the latest generation wide-pore SPPs, superior efficiency can be achieved for proteins RP separations, but there are still some remaining issues, namely: (1) the strong adsorption of large proteins on silica-based materials and (2) the lack of selectivity between closely related protein species [22,23]. To this end, interesting insights have been gleaned to better appreciate the appeal of phenyl surface chemistries over the alkyl bonded phases that have near invariably been used for protein RPLC separations. Amgen scientists have published multiple times on the utility of columns based on a so-called diphenyl bonding [24,25]. In this study, we have systematically characterized the performance of a new wide-pore silica-based SPP material with even higher phenyl coverage. This new material exhibits a novel surface chemistry that is synthesized using a multistep silanization process to yield a phenyl-based bonded phase which is both inordinately high in coverage (at 6 μmol phenyl moiety/m^2) and comprised of rigidly constrained carbons. This material is believed to limit silanol interactions by extensively masking the base particle, to facilitate more discrete desorption by minimizing the conformational heterogeneity of protein adsorption, and to improve resolving power by being highly retentive. In addition, it is believed to afford advantageous selectivity through possible π-π interactions and steric effects that are not present in common silica-based materials (butyl, octyl or octadecyl phases). Column efficiency, recovery, selectivity and the possibility to use mass spectrometry (MS) compatible mobile phase have been evaluated for this column against other recently developed wide-pore RPLC technologies as applied to detailed analyses of mAbs and ADCs.

2. Experimental

2.1. Chemicals and samples

Acetonitrile and water were purchased from Fisher Scientific (Reinach, Switzerland). Trifluoroacetic acid (TFA), formic acid (FA), dithiothreitol (DTT) and tris(hydroxymethyl)aminomethane (TRIS) were purchased from Sigma-Aldrich (Buchs, Switzerland). IdeS (FabRICATOR®) was purchased from Genovis AB (Lund, Sweden). FDA and EMA approved monoclonal antibody (palivizumab, ofatumumab and panitumumab) and antibody-drug conjugate (brentuximab vedotin) samples were kindly provided by the Center of Immunology Pierre Fabre (Saint-Julien-en-Genevois, France). NIST mAb (NIST Reference Material 8671) was obtained from the National Institute of Standards and Technology (Gaithersburg, MD, USA). Reduced, IdeS digested NIST mAb was obtained from Waters (mAb Subunit Standard, Milford, MA, USA).

2.2. Chromatographic system and columns

Measurements were performed on a Waters Acquity UPLC I-Class system equipped with a binary solvent delivery pump, an autosampler, UV and fluorescence (FL) detector. The system includes a flow through needle (FTN) injection system with 15 μL needle and a 0.5 μL UV and 2 μL FL flow-cell. Data acquisition and instrument control were performed by Empower Pro 3 software (Waters).

The high coverage phenyl bonded wide-pore superficially porous particle reversed phase column (150 mm × 2.1 mm, BioResolve RP mAb Polyphenyl, 2.7 μm, 450 Å) was provided by Waters (Milford, MA, USA). The other reference columns employed in this study for comparison purpose were the Aeris Widepore XB-C18 (150 mm × 2.1 mm, 3.6 μm, 300 Å), MabPac RP (100 mm × 2.1 mm, 4 μm, 1500 Å), HALO Protein C4 (150 mm × 2.1 mm, 3.4 μm, 400 Å), Protein BEH 300 C4 (150 mm × 2.1 mm, 1.7 μm, 300 Å) and AdvanceBio RP-mAb C4 (150 mm × 2.1 mm, 3.5 μm, 450 Å), purchased from Phenomenex (Torrance, CA, USA), Thermo Fisher Scientific (Waltham, MA, USA), Advanced Materials Technology (Wilmington, DE, USA), Waters (Milford, MA, USA) and Agilent (Santa Clara, CA, USA), respectively.

2.3. Sample and mobile phase preparation

To evaluate and compare the kinetic efficiency, recovery and selectivity of the columns, mAbs and ADC samples were analyzed at intact and sub-unit levels. Intact therapeutic proteins were diluted

to 1 mg/mL with water and injected without further preparation. Preparation of protein sub-units was performed using the 1 mg/mL solutions of intact proteins. MAb samples were reduced by adding 10 μL of freshly prepared 1 M DTT to 90 μL 1 mg/mL protein (to have 100 mM DTT in the final solution) and incubating the solution at 45 °C for 30 min. The ADC sample was reduced by adding 10 μL of freshly prepared 100 mM DTT to 90 μL 1 mg/mL protein (to have 10 mM DTT in the final solution) and incubating the solution at 30 °C for 60 min. After reduction, samples were kept at 4 °C. For the evaluation of selectivity, NIST mAb was digested by IdeS enzyme and then reduced by DTT. IdeS cleaves a mAb under its inter-chain disulfides of the hinge region resulting in Fc/2 (or single chain Fc, sFC) and F(ab')$_2$ fragments. The resulting F(ab')$_2$ fragment can be further deconstructed to light chain (LC) and Fd' sub-units, by chemical reduction [26]. After this combined sample preparation of IdeS digestion and reduction, the sample contains Fc/2, LC and Fd' fragments. The resulting pool of these ~25 kDa fragments is favorable for chromatographic and mass spectrometric characterization [27].

100 U lyophilized IdeS enzyme (one well of a 96 well plate format) was reconstituted in 40 μL TRIS (pH 7.5). 20 μL of this IdeS solution (50 U) was added to 50 μL 1 mg/mL mAb solution. Samples were incubated and mixed at 45 °C for 30 min. After digestion, samples were reduced by adding 8 μL of freshly prepared 1 M DTT solution (to have approximately 100 mM DTT concentration in the sample). Reduction was performed at 45 °C for 30 min. After sample preparation, samples were kept at 4 °C.

Mobile phase A was 0.1% TFA (v/v) in water, mobile phase B was 0.1% TFA (v/v) in acetonitrile, unless indicated otherwise. A volume of 1 μL was injected using linear gradients and various gradient conditions (see detailed information at the corresponding sections). Temperature varied between 60 and 90 °C, and flow rate was set to 0.3 mL/min and 0.6 mL/min, respectively. Data were acquired using 280 nm excitation and 360 nm emission wavelengths with 20 Hz sampling rate. Data were processed using Excel and Drylab (4.2) software.

2.4. Apparatus and methodology

2.4.1. Column efficiency, peak capacity, separation impedance

For studying and comparing column performance, intact and reduced NIST mAb were injected and the peak widths of the native, heavy chain and light chain peaks were measured.

The column efficiency in gradient elution mode is generally described by the peak capacity [28,29]. For the comparison of column efficiency in gradient elution mode, several theoretical and experimental expressions can be found in the literature [30–34].

To have comparable results with the studied columns (different dimensions, porosity, phase ratio) at different flow rates, the rules of LSS theory and geometrical method transfer were applied [35,36]. The next formula was used to calculate the gradient steepness (s) for the given conditions:

$$s = (\phi_e - \phi_0) \cdot \left(\frac{L}{t_g - t_0}\right) \cdot u = \beta \cdot L \cdot u_0 \quad (1)$$

where Φ_0 is the initial mobile phase composition and Φ_e is the final mobile phase composition, L is the column length, t_g and t_0 are the gradient time and column dead time, u_0 is the linear velocity and β is the so-called time steepness of the linear gradient.

Linear velocity and column total porosity (ε_T) were determined by injecting uracil as t_0 indicator; and the next formula was used:

$$u_0 = \frac{L}{t_0} = \frac{4F}{\varepsilon_T d_c^2 \pi} \quad (2)$$

Where F is the flow rate and d_c is the column diameter. For the peak capacity measurements, the solvent strength was varied linearly with gradient times. On 150 mm long columns, t_g was varied between 5 and 40 min, while on the 100 mm long column it was set between 3.5 and 30 min in 5 min steps. Two flow rates were applied (F_1 = 0.3 mL/min and F_2 = 0.6 mL/min). Peak capacities were experimentally determined on the basis of gradient time, column dead time and the average peak widths measured at 50% height ($w_{50\%}$). The following equation was used to estimate the peak capacity based on peak widths at 4σ, corresponding to a resolution of Rs = 1 between consecutive peaks:

$$n_c = 1 + \frac{t_g - t_0}{1.699 \cdot w_{50\%}} \quad (3)$$

The experimentally observed peak capacity (n_C) values are not directly comparable, since peak capacity depends on column length. Therefore, the peak capacities extrapolated to 1 m column length ($n_{C.M}$) were considered in this comparison. When maintaining constant the gradient steepness, the following formula can be written:

$$n_{c,M} = n_c \sqrt{\frac{100}{L}} \quad (4)$$

During the experiments Φ_e-Φ_0 was kept constant (15%) for all columns. But for maintaining similar apparent retention on the different stationary phases, Φ_0 was set at 30%B on most columns, except on the AdvanceBio RP MAb C4 column, where Φ_0 was set at 25%B.

When studying the efficiency, peak capacity *vs.* gradient time plots (n_c – t_g) and peak capacity *per* meter versus gradient span (expressed in time/column length dimension such as min/meter) plots ($n_{c,M}$ – S_g) were compared. The gradient span (S_g) in this case was calculated as:

$$S_g = t_g \left(\frac{100}{L}\right) \quad (5)$$

The column performance also depends on column permeability (K_v) and retention time, the latter being related to column dead time and/or gradient time. Therefore, peak capacity plots do not give information about the overall quality of the separation (e.g. achievable separation time), but only about the reachable peak widths. By analogy to Knox's separation impedance concept [37], similar representation of kinetic performance can be constructed by calculating the peak capacity *per* unit time and *per* unit pressure values, according to the next formula [16,38,39]:

$$PPT = \frac{n_c}{t_g \cdot \Delta P} \quad (6)$$

where PPT is the peak capacity *per* unit time and *per* unit pressure value and ΔP is the column pressure drop (the maximum pressure measured during the gradient program, corrected for extra-column pressure drop). Plots of PPT as a function of gradient steepness were constructed and compared for two sets of linear velocity. Column permeability (K_v) was experimentally determined, using the following relationship:

$$K_V = \frac{u_0 \cdot \eta \cdot L}{\Delta P} \quad (7)$$

where η is the mobile phase viscosity, ΔP is the experimentally observed column pressure drop.

2.4.2. Recovery and the effect of mobile phase temperature

On-column adsorption of intact mAbs and their heavy chain and light chain sub-units was evaluated in a systematic way. Short gradient runs (5 min) were carried out on four different types of stationary phases (including silica-, polymer- and hybrid-based materials) at a series of temperature as T = 60, 65, 70, 75, 80, 85

and 90 °C. The flow rate was set to 0.6 mL/min, a volume of 1 μL was injected and FL detection (excitation at 280 nm, emission at 360 nm, 20 Hz) was used. The gradient was set as 30–45% B on all columns, except on the MAbPac RP column (29–44% B). This way, all the species eluted with appropriate retention at all temperatures and on each column.

To compare the adsorption of proteins on the different stationary phases, the recovery of intact, heavy- and light chain sub-units of NIST mAb, palivizumab, ofatumumab and panitumumab were determined. NIST mAb was selected because it is standard reference material that can be easily obtained. Panitumumab is one of the worst case mAbs, while ofatumumab represents an average mAb and palivizumab is the best case mAb, in terms of on-column adsorption [23].

The relative peak areas (expressed as recovery percentage) related to the values observed at the highest temperature on the prototype column were plotted as a function of temperature. Since the largest peak areas were observed at the highest temperature, the relative recovery can be determined and its temperature dependence can be shown.

2.4.3. Selectivity, method optimization

To study the selectivity of the prototype column, the chromatograms obtained for NIST mAb and brentuximab vedotin sub-units were compared to other columns when operating all of them under their individual optimal conditions. The optimal conditions were determined on the basis of resolution models built from 4 initial experiments (t_g-T model) [40]. For the NIST mAb sample, gradient times were set as t_{g1} = 5 and t_{g2} = 15 min, while for the brentuximab vedotin t_{g1} = 10 and t_{g2} = 20 min were chosen. Temperature was set at two levels in both cases as T_1 = 70 and T_2 = 90 °C. Flow rate was set to F = 0.6 mL/min and 1 μL sample was injected. Based on the critical resolution maps, the optimum working points (WP) were found and experiments were run under the WP conditions.

2.4.4. Mobile phase additives

Residual silanols are known to contribute in a non-negligible way to the overall selectivity of the stationary phase in RPLC [41]. On the other hand, acidic silanols can result in pronounced adsorption due to strong (presumably ionic) interactions even under highly acidic conditions. Indeed, cation exchange activity of RPLC materials was even observed when using 0.1% TFA in the mobile phase (pH around 2) [16,17]. TFA is a frequently used ion-pairing additive for the RPLC of proteins as it protonates basic residues and forms ion pairs with the protein [12]. This ion-pair reduces unwanted interactions with the stationary phase and possesses desirable chromatographic properties. However, the formation of stable ion-pairs should be avoided when MS detection is applied. Indeed, ion-pairing additives, such as TFA suppress ionization in the source, leading to sensitivity loss up to an order of magnitude or more, depending on the sample and the MS conditions [12]. Thus, the possibility to –even partially- replace TFA with other additives which do not form stable ion-pairs, such as FA would be welcomed. The effect of partial replacement of TFA with FA in the mobile phase on the kinetic efficiency and recovery was evaluated and compared to what can be observed on the HALO C4 silica based SPP material. For this comparison reduced, IdeS digested NIST mAb and reduced brentuximab vedotin were used. 0.1% TFA, 0.05% TFA + 0.05% FA, 0.02% TFA + 0.08% FA and 0.01% TFA + 0.09% FA (v/v) were used as mobile phase additives. Linear gradients were run from 26 to 49%B in 18.4 min for the ADC fragments and from 25 to 42%B in 17 min for the mAb fragments. The recovery of the most critical, highly hydrophobic triply loaded heavy chain (H3) of the ADC was evaluated. Average peak capacity calculated from the widths of the six major ADC peaks were also compared when using different mobile phase additives on the HALO Protein C4 column versus the high coverage phenyl bonded wide-pore SPP column.

3. Results and discussion

3.1. Peak capacity and separation impedance

A systematic study was carried out to determine the peak capacity and gradient separation impedance (PPT) of various wide-pore SPP materials. Table 1 summarizes the physical properties of the columns used in this comparison. In practice, proteins are generally separated in gradient elution mode at elevated temperature. Elevated temperature is beneficial, because it decreases the strength of secondary ionic interactions between residual silanols and positively charged biomolecules [22,23]. Moreover, the use of high temperature strongly enhances analyte diffusion. Furthermore, an ion-pairing reagent, namely TFA, was systematically added to the mobile phase to improve peak shape in the case of protein separation. To best emulate typical use conditions, a column temperature of 80 °C was employed, 0.1% TFA was added to the mobile phase and gradient spans were varied from between S_g = 23 and 267 min/meter, which are fairly common in the current practice. (For better understanding, this S_g range corresponds to gradient times ranging between 5 and 40 min for a 150 × 2.1 mm column at 0.3–0.6 mL/min flow rate). The chromatography of several test compounds, including intact NIST mab (~150 kDa) and its heavy- (~50 kDa) and light chain (~25 kDa), was investigated as a function of gradient steepness and linear velocity. These experimental variables are directly related to the mobile phase flow-rate and the gradient time duration which are often used to optimize a separation in practical work. The former has a direct influence on the peak width, while gradient duration plays an important role on the resolution as it affects the retention factor of the solute in the mobile phase composition upon elution. It should be stressed that these conditions are not meant to maximize the peak capacity for any particular column or compound, since higher peak capacity can sometimes be achieved by choosing longer gradient times or lower flow rates. Instead, we merely wanted to identify a set of conditions to allow a fair comparison within a practically acceptable time frame.

Table 1
Physical properties of the columns used in this study.

Column	base	dimension	pore diameter (Å)[a]	d (μm)	*rho*	ε_t	*Kv* (cm^2)
BioResolve RP mAb Polyphenyl (Waters)	silica	150 × 2.1 mm	450	2.7	0.70	0.65	1.4×10^{-10}
BEH 300 C4 (Waters)	ethylene-silica hybrid	150 × 2.1 mm	300	1.7	0	0.70	5.8×10^{-11}
HALO Protein C4 (AMT)	silica	150 × 2.1 mm	400	3.4	0.88	0.58	2.6×10^{-10}
AdvanceBio RP-mAb C4 (Agilent)	silica	150 × 2.1 mm	450	3.5	0.83	0.56	1.8×10^{-10}
MAbPac RP (Thermo)	divinylbenzene polymer	100 × 2.1 mm	1500	4.0	0	0.71	9.4×10^{-11}
Aeris WP C18 (Phenomenex)	silica	150 × 2.1 mm	200	3.6	0.87	0.52	2.1×10^{-10}

* *rho* denotes the ratio of the diameter of the core to the diameter of the particle, ε_t signifies the total porosity and *Kv* defines the permeability.

[a] Pore diameters have been measured for these materials by several different approaches. Mercury injection porosimetry was used in place of nitrogen BET for BioResolve RP mAb Polyphenyl particles to ensure accurate measurement of large pores.

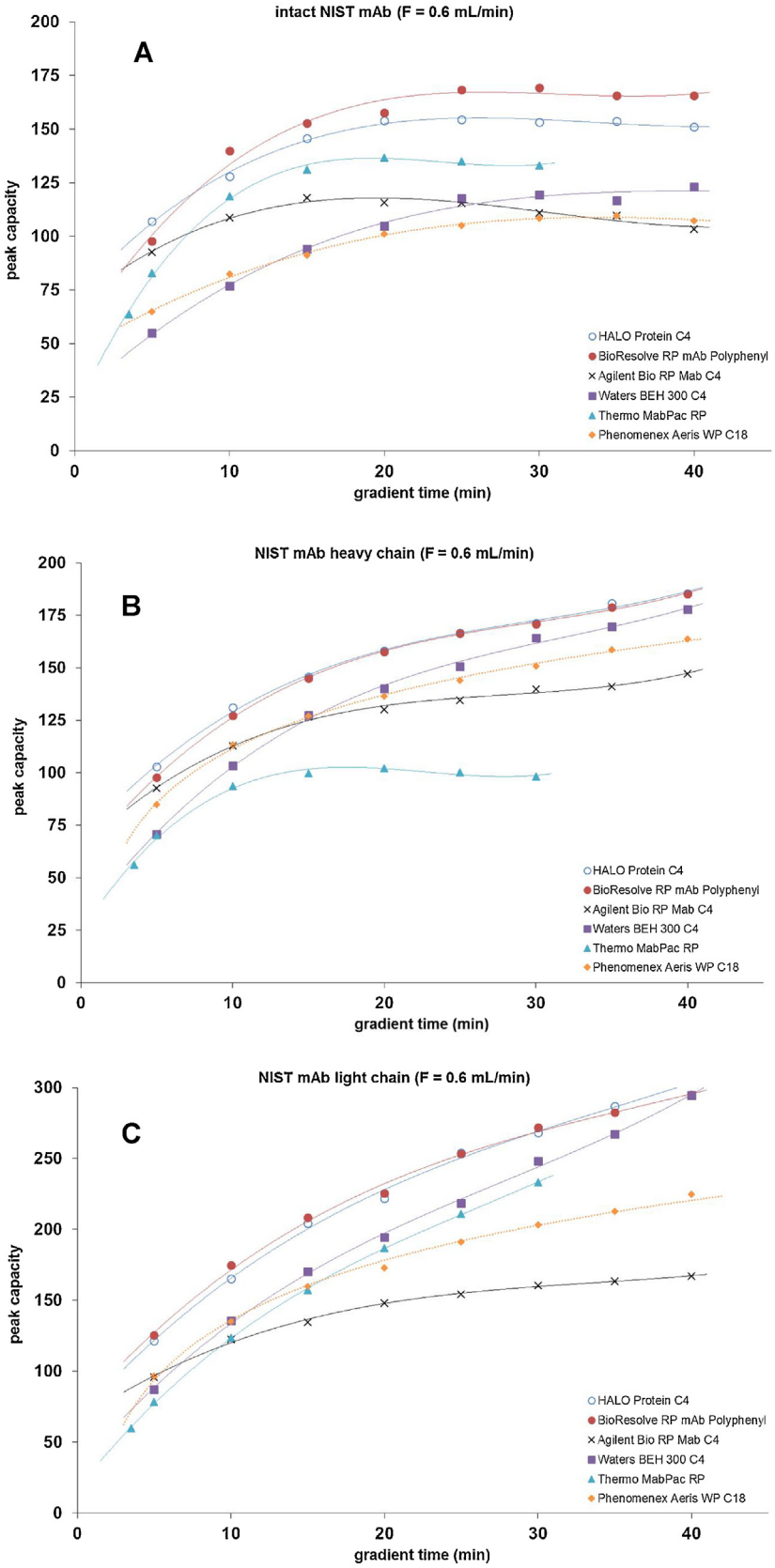

Fig. 1. Peak capacity versus gradient time plots of intact NIST mAb (A) and its heavy- (B) and light chains (C) observed at a flow rate of 0.6 mL/min, temperature of 80 °C and with $\Delta\Phi = 0.15$.

Fig. 1 shows the observed peak capacity values *vs.* applied gradient time for $F = 0.6$ mL/min. When the gradient time was longer than 10 min, the BioResolve RP mAb Polyphenyl column outperformed all the other columns for the intact NIST mAb sample (Fig. 1A). Peak capacity between $n_c = 100$ and 175 were observed. The HALO Protein C4 protein column showed slightly lower efficiency ($n_c = 100$–150), followed by the MabPac RP column ($n_c = 100$–130). The other three columns (AdvanceBio RP Mab C4, BEH 300 C4 and Aeris WP C18) performed $n_c < 120$ under these conditions. For the heavy chain of NIST mAb (Fig. 1B), the BioResolve RP mAb Polyphenyl and HALO Protein C4 protein columns yielded the highest (and similar) peak capacity ($n_c = 100$–180), while the Thermo MabPac RP column provided the lowest efficiency ($n_c < 95$). For the smallest fragment (light chain of NIST mAb), it was again the BioResolve RP mAb Polyphenyl and HALO Protein C4 columns that showed the highest efficiency ($n_c = 120$–300) (Fig. 1C). For this fragment, the Agilent BioRP Mab C4 column gave the lowest peak capacity ($n_c = 95$–170). One possible reason for the excellent efficiency of the prototype and the HALO C4 protein columns is that they possess the largest average pore size (450 Å) among all the SPP materials. As already discussed, a large pore diameter is known to be beneficial for large proteins [1,18]. The MabPac RP column possesses an even larger pore size (1500 Å), but is a fully porous polymeric-based material with a relatively large particle size (4 μm). Probably, this could be the reason why it shows moderate peak capacity (proteins have longer residence time in the inter particle volume). However, it should be noted that nominal average pore diameters defined by various manufacturers should be interpreted with caution as they are based on different methodologies (e.g. gas adsorption/desorption, mercury intrusion or inverse size exclusion chromatography). Obviously, weaker secondary interactions (due to the lack of residual silanols) on the MabPac RP column can also improve the apparent efficiency. However the impact of secondary interactions on efficiency is hard to estimate and dissociate from other sources of band-broadening [17]. Very similar behavior and ranking of columns were observed at 0.3 mL/min, except that the absolute peak capacity was somewhat lower compared to 0.6 mL/min (data not shown).

Fig. 2 highlights the obtained peak capacity per meter values as a function of gradient span at 0.6 mL/min for all columns. The ranking of the columns in this comparison is quite similar to the previous one, except for the MabPac RP column since this column is not available in a 150 mm long format (only in a 100 mm length). When the efficiency is calculated for 1 m long columns, the performance of the MabPac RP column was more favorable. In all, the BioResolve RP mAb Polyphenyl column and the HALO Protein C4 columns produced the highest peak capacity for NIST mAb and its fragments. A maximum peak capacity per meter of $n_{c,M} \sim 440$, 480 and 760 were observed with the BioResolve column for the intact NIST mAb, its heavy chain and its light chain, respectively.

Another representation of column capability is shown in Fig. 3. In this case, separation quality was judged on the basis of peak capacity, column permeability and analysis time, simultaneously. Fig. 3A shows the peak capacity *per* pressure and time unit (PPT) values as a function of the gradient span at $F = 0.6$ mL/min, and 80 °C for all columns. In this representation, the higher the PPT value, the lower the "separation impedance" is. These plots illustrate which columns are most amenable to being used to achieve faster separations at low pressure and thus their amenability to being taken advantage of on all types of LC instrumentation. By this performance metric, the HALO Protein C4 column appears to be exemplary, because of its high permeability ($K_v = 2.6 \times 10^{-10}$ cm^2) and peak capacity. The BioResolve column can be ranked as having the next best separation impedance. Indeed, it provides the highest peak capacity in most cases, but it also exhibits two times lower permeability compared to the HALO Protein C4 column (which is logical when considering the particle diameters). Generally, the BEH 300 C4 column provides the highest separation impedance, due to its low permeability. The same conclusion was drawn at a lower, 0.3 mL/min flow rate, but obviously the *PPT* values were higher, due to the lower operating pressure compared to $F = 0.6$ mL/min.

3.2. On-column protein adsorption – effect of temperature

Temperature is known to play a crucial role in the RPLC analysis of proteins [22,23]. First of all, it is generally mandatory to work at elevated temperatures (e.g. 80–90 °C) to attain appropriate recovery, especially when proteins are analyzed at the intact level. At lower temperatures, proteins may adsorb too strongly or too heterogeneously onto the stationary phase, resulting in asymmetric, tailed peaks or even incomplete elution. On the other hand, elevated temperature may increase the risk of on-column protein degradation, particularly for longer gradients. Indeed, harsh eluent conditions generally used in RPLC (high temperature, strongly acidic mobile phase and longer residence times) may accelerate the cleavage of the protein backbone. Consequently, it is important to critically evaluate the effect of temperature when developing RPLC methods for proteins. The use of lower temperature could decrease the risk the on-column degradation and extend column lifetime, but adsorption has to be kept reasonable.

The adsorption-desorption properties of the high coverage phenyl bonded silica SPP material (BioResolve RP mAb Polyphenyl) were compared to commercial reference materials of silica (HALO Protein C4), hybrid silica (BEH 300 C4) and polymer (MabPac RP) particles at various temperatures.

At their intact level, all of the tested mAbs – except panitumumab – showed excellent recovery (above 90%) on both columns within the entire temperature range studied, from 60 to 90 °C (data not shown). The same was observed for the light and heavy chains of those mAbs. Adsorption of panitumumab, as being the most problematic mAb, is shown in Figs. 4 and 5. Fig. 4 shows how elution profiles change when decreasing temperature on the prototype and on the reference silica material, namely the HALO Protein C4 phase. With the BioResolve column, temperature can be decreased to 80 °C while still achieving >90% recovery of the intact mAb on the BioResolve column, and it is even possible to work at 70 °C to satisfactorily recover the heavy chain and 60 °C for the light chain. On the contrary, a temperature of 85–90 °C is systematically required on the HALO column to achieve reasonable recovery for these different samples (Fig. 4).

For the analysis of mAbs at their intact level, the column technologies can be ranked in terms of recovery as follows: polymeric high coverage phenyl bonded silica > C4 bonded hybrid > C4 bonded silica material (Fig. 5). Note that the BioResolve column is a silica-based material, showing comparable recovery to the polymeric one, down to 80 °C and clearly outperforming the BEH and HALO columns. Interestingly, recovery of the panitumumab heavy- and light chains are very similar on the BioResolve and MAb Pac RP columns. More than 94% of the light chain is recovered through the entire temperature range (60–90 °C), and above 90% of the heavy chains were recovered above 70 °C. Recoveries on the BEH and HALO materials were significantly lower. Thus, at the sub-unit level, recovery from the materials can be ranked as follows: polymeric ≈ high coverage phenyl bonded silica > C4 bonded hybrid > C4 bonded silica material.

3.3. Selectivity and method optimization for NIST mAb and brentuximab vedotin

In most forms of RPLC, interactions with the stationary phase are predominantly mediated through hydrophobic interactions

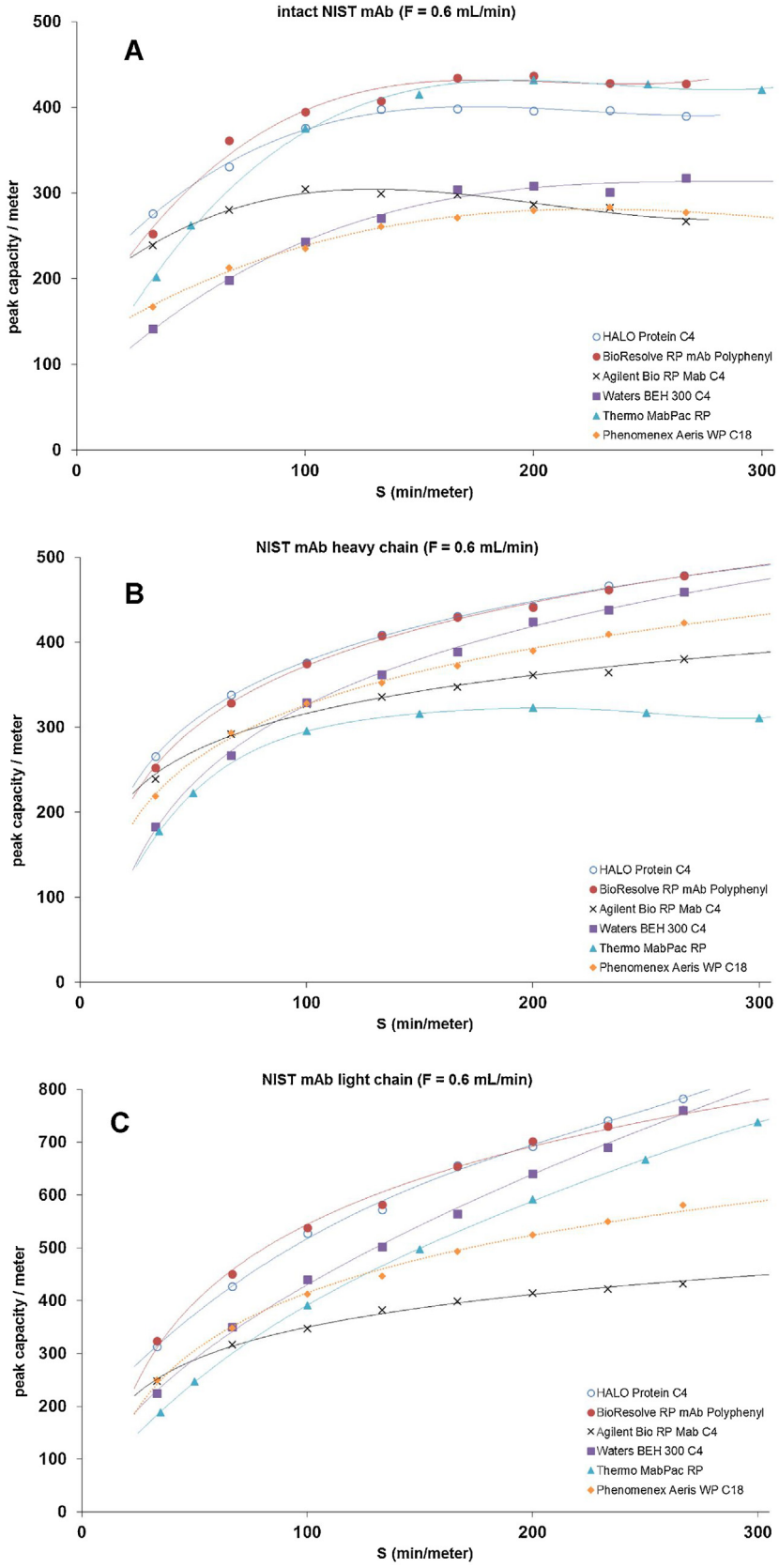

Fig. 2. Peak capacity versus gradient steepness plots related to 1 m column length of intact NIST mAb (A) and its heavy- (B) and light chains (C) observed at a flow rate of 0.6 mL/min, temperature of 80 °C and with $\Delta\Phi = 0.15$.

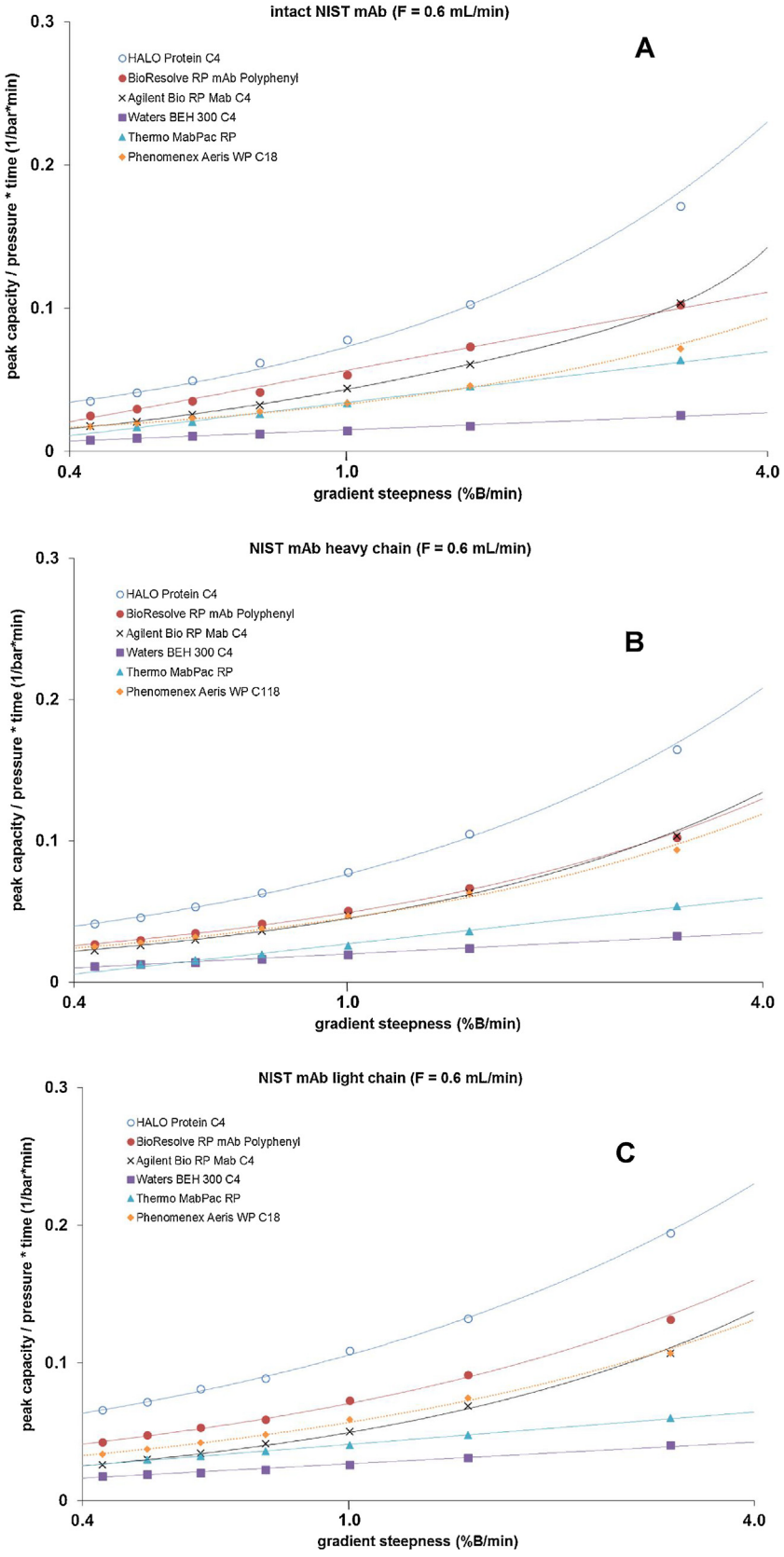

Fig. 3. Peak capacity per pressure and time unit versus gradient steepness plots of intact NIST mAb (A) and its heavy- (B) and light chain (C) observed at a flow rate of 0.6 mL/min, temperature of 80 °C and with $\Delta\Phi = 0.15$.

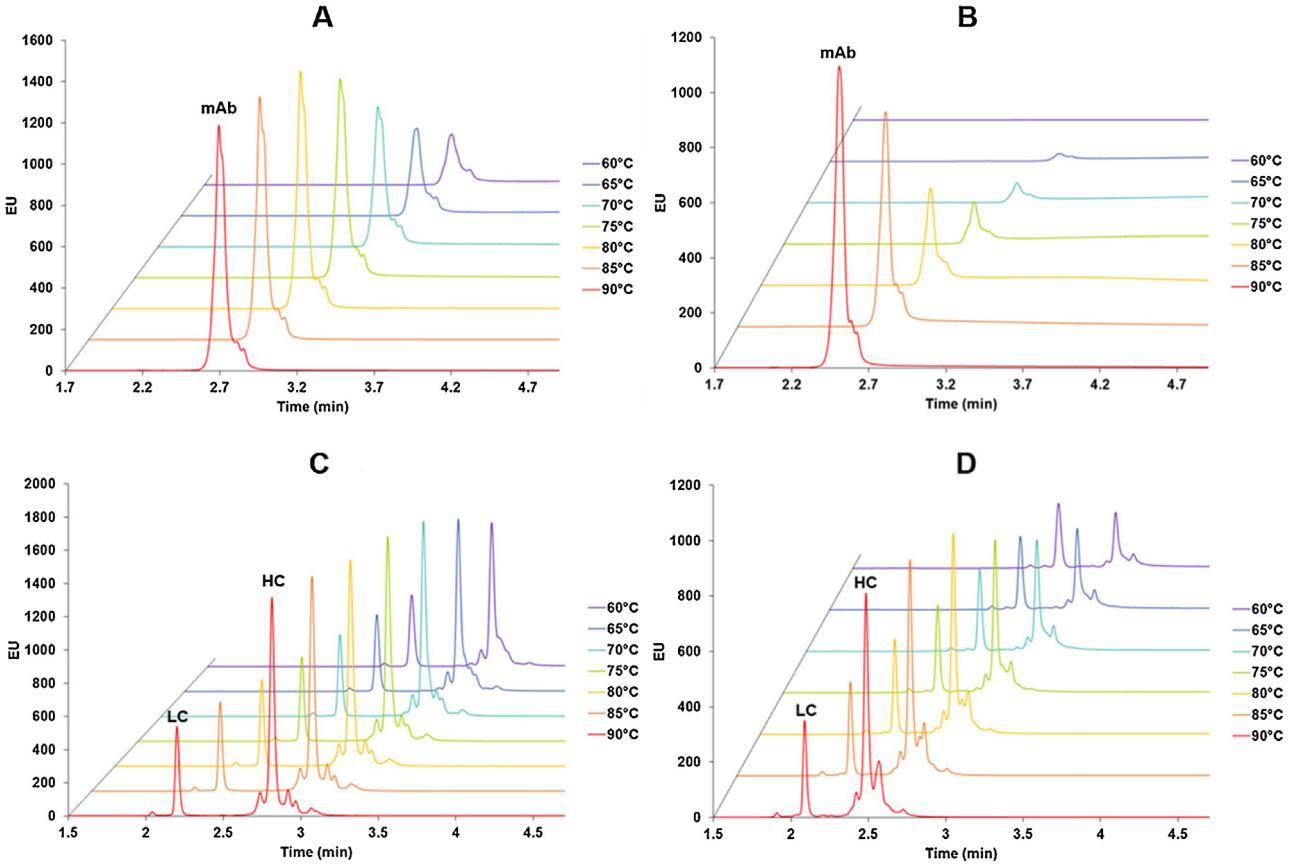

Fig. 4. Chromatograms of panitumumab on the BioResolve RP mAb Polyphenyl (A, C) and the Halo Protein C4 columns (B, D) at various temperatures. Recovery was evaluated at intact (A, B) and subunit levels (C, D) by reducing the mAb to obtain the heavy- and light chains. Gradient: 25–40%B in 5 min, mobile phase A: 0.1% TFA in water, B: 0.1% TFA in acetonitrile. Flow rate: 0.6 mL/min, injection volume: 1 μL. Detection: FL_{ex}: 280 nm, FL_{em}: 360 nm, 20 Hz.

between the nonpolar amino acid residues of proteins and immobilized ligands (typically C4, C8 or C18). Accordingly, solutes tend to elute in their order of increasing molecular hydrophobicity. Nevertheless, cation-exchange through residual silanols is not negligible for proteins, even when using 0.1% TFA as additive [16,17]. That is to say there are a number of factors that contribute to the selectivity of a protein RPLC column and that the most obvious way to affect selectivity is to manipulate the surface chemistry of a stationary phase. As mentioned earlier, the BioResolve RP mAb Polyphenyl stationary phases synthesized by a multistep silanization process that yields a phenyl-based bonded phase that is both high in coverage (at 6 μmol phenyl moiety/m^2) and comprised of rigidly constrained carbons. These attributes are likely to be of significant influence to the retention and selectivity of proteins due to steric and potentially even π-π interactions that are otherwise not present with alkyl bonded phases. These effects are likely to be quite prominent given that proteins tend to contain a multitude of aromatic amino acids [42–46]. Moreover, the accessibility to residual silanols are probably less important, compared to common alkyl ligands, due to the steric hindrance imposed by this new bonded phase.

The linear solvent strength model (LSS) is a widely accepted theory which describes analyte retention as a function of the volume fraction (Φ) of elution solvent. This model has worked well to describe the retention of numerous types of analytes, including large proteins such as mAbs or mAb sub-units [40].

Besides gradient programming, the other most important method variable for optimizing protein RPLC is mobile phase temperature. However, with large biomolecules, the effect of temperature on retention becomes more complex. Depending on the stability of the secondary structure, the molecules unfold to various extents and hence interact with the stationary phase with various strengths [47]. Due to the different conformation-dependent responses of proteins at elevated temperatures, the change in retention can be very different [48,49]. Another issue related to temperature is the possible thermal degradation of proteins when working at elevated temperature. It was shown for mAbs that analysis time should be kept below 20 min to avoid degradation at 70–90 °C [22].

Table 2
Optimal conditions (working points) for selectivity comparison.

	NISTmAb		brentuximab vedotin	
Column	t_g (min)	T (°C)	t_g (min)	T (°C)
Waters BioResolve RP mAb Polyphenyl	15	90	20	90
Waters BEH 300 C4	15	86	10.5	86
HALO Protein C4	15	86	20	90
Thermo MAbPac RP	10	77	13.3	90
Phenomenex Aeris WP C18	15	85	14	90

All the above discussed points were considered to optimize separation conditions for resolving components of reduced, IdeS digested NIST mAb and reduced brentuximab vedotin. A general approach is to simultaneously model the effect of temperature and gradient steepness (s) [40]. Optimal conditions were determined for both samples on five different columns, and the corresponding chromatograms are shown in Fig. 6, while the conditions are summarized in Table 2. Please note that in Fig. 6, the chromatograms are shown as function of apparent retention factor (k_{app}) to be comparable (since column length and porosity were not identical). An

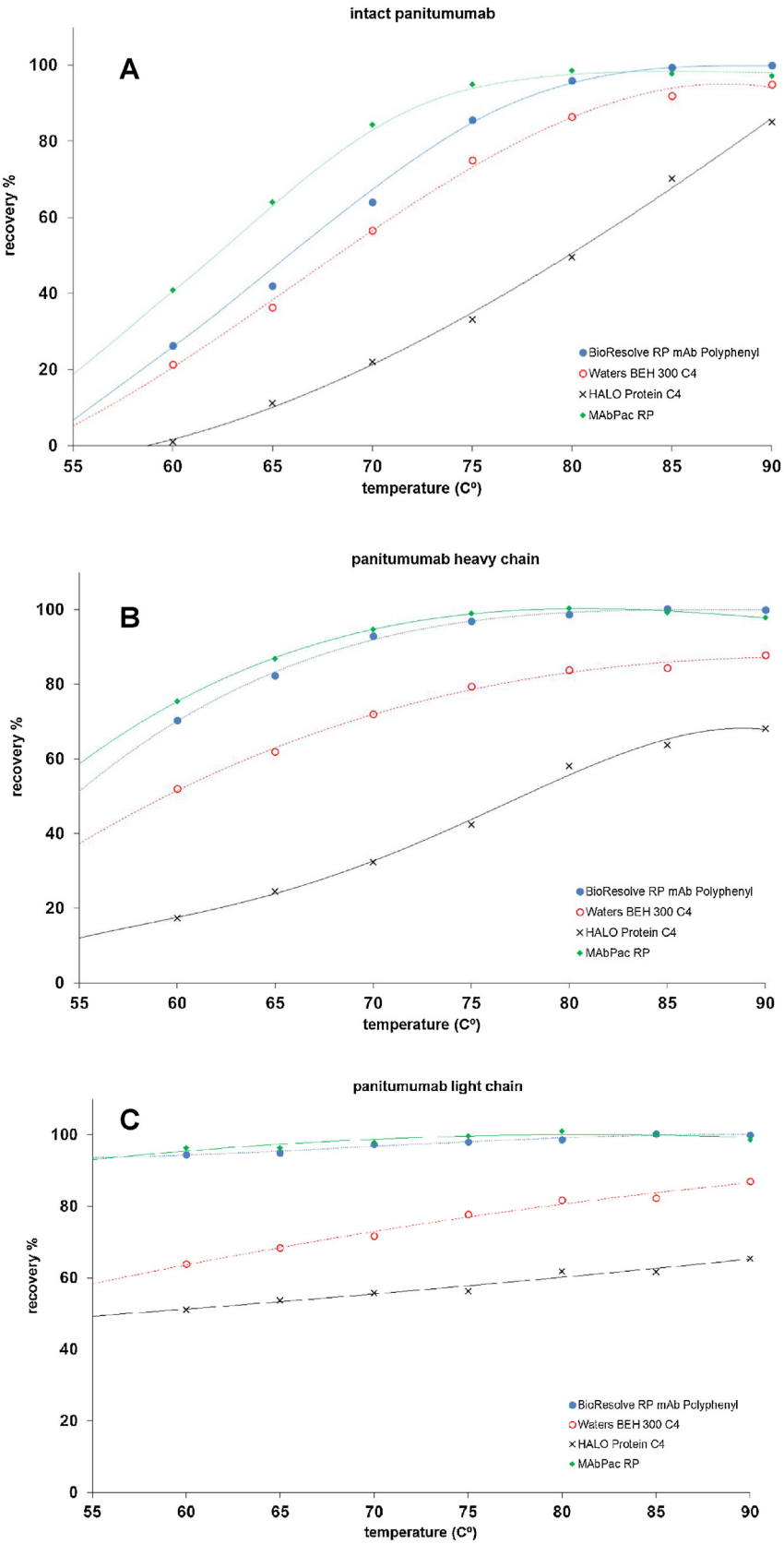

Fig. 5. Relative recovery of intact panitumumab (A) and its heavy chain (B) and light chain (C) as a function of temperature on different stationary phases.

important finding is, that on the BioResolve column, the selectivity between the Fc/2 and LC peaks of NIST mAb is significantly greater than on other columns. In turn, the BioResolve column resolves additional peaks in the separation space between them (Fig. 6A, red circle). These minor peaks (variants) were not separated on the other columns, no matter the condition under which they were

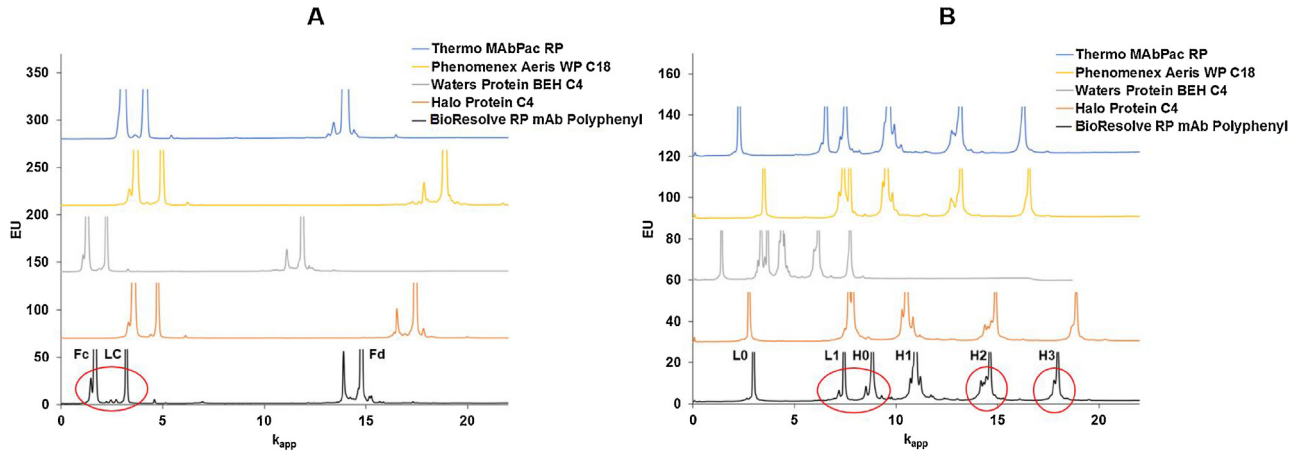

Fig. 6. Chromatograms of reduced, IdeS digested NIST mAb (A) and reduced brentuximab vedotin (B) using optimized conditions on each column. Optimal conditions were determined using Drylab 4 software and are detailed in section 2.4.3. Red circles highlight the resolution of Fc/2 and LC species of NIST mAb and L1/H0, H2 and H3 species of brentuximab vedotin on the BioResolve RP mAb Polyphenyl column. (For interpretation of the references to colour in this figure legend, the reader is referred to the web version of this article.)

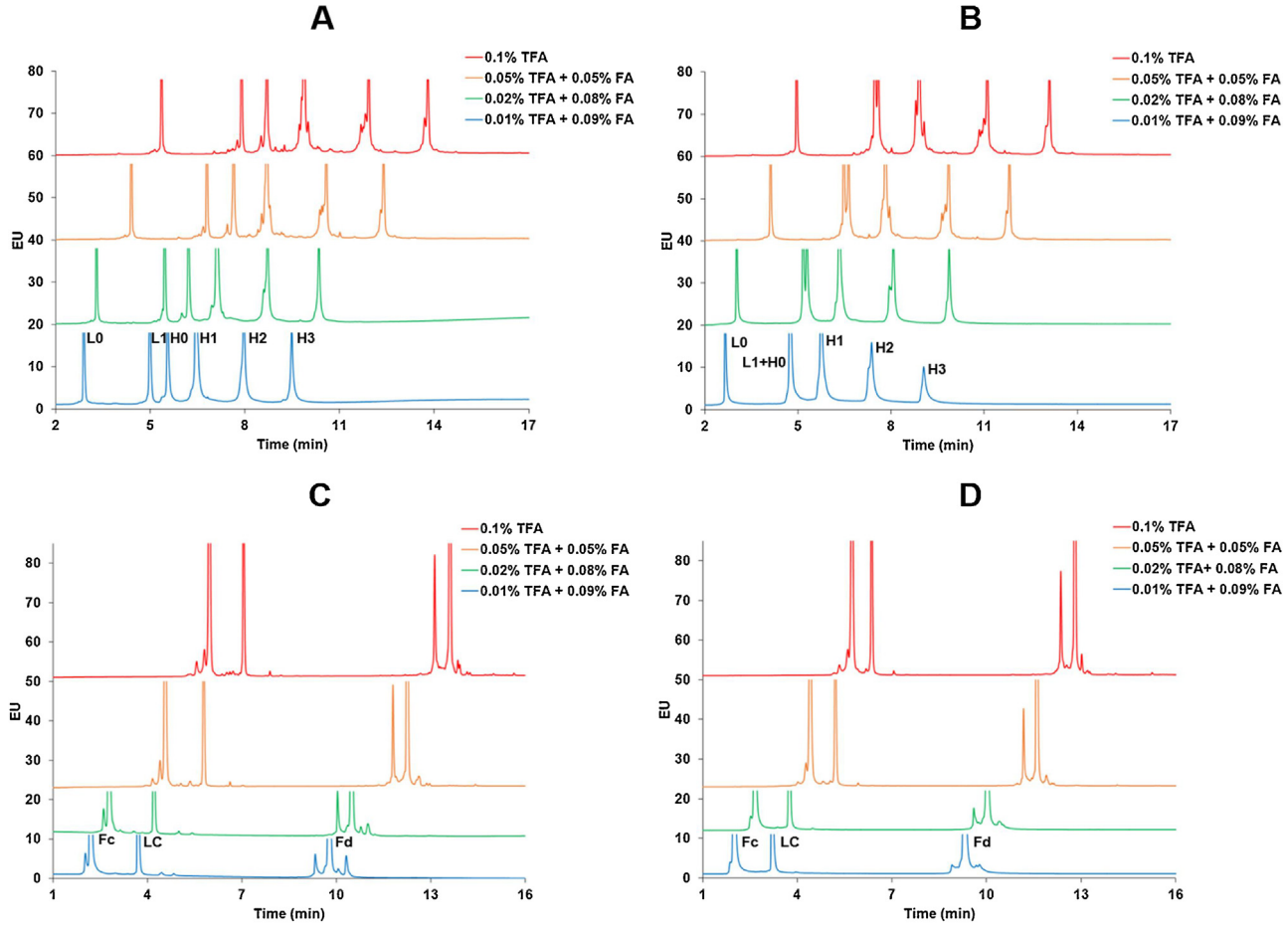

Fig. 7. Chromatograms of reduced brentuximab vedotin observed with the BioResolve RP mAb Polyphenyl (A) and the HALO Protein C4 (B) columns, and chromatograms of reduced, IdeS digested NIST mAb with the BioResolve RP mAb Polyphenyl (C) and HALO Protein C4 (D) columns using various TFA/FA concentrations. Gradient: 26–49%B in 18.4 min for the ADC fragments and 25–42%B in 17 min for the mAb fragments, mobile phase A: water and B: acetonitrile containing various TFA/FA concentrations. Temperature: 90 °C, flow rate: 0.6 mL/min, injection volume: 1 μL. Detection: FL_{ex}: 280 nm, FL_{em}: 360 nm, 10 Hz.

used. The least favorable selectivity was observed with the polymeric column (MAbPac RP), and the other columns provided more or less the same separation quality.

There are two objectives when analysing a cysteine linked ADC sample, like brentuximab vedotin, by RPLC. The first is to separate the various payload bearing versus unconjugated species so that it might be possible to determine the average drug to antibody ratio (DAR), an important quality attribute of an ADC. Among these species, it is quite critical and often challenging to resolve the light chain with one payload (L1) from the unconjugated heavy

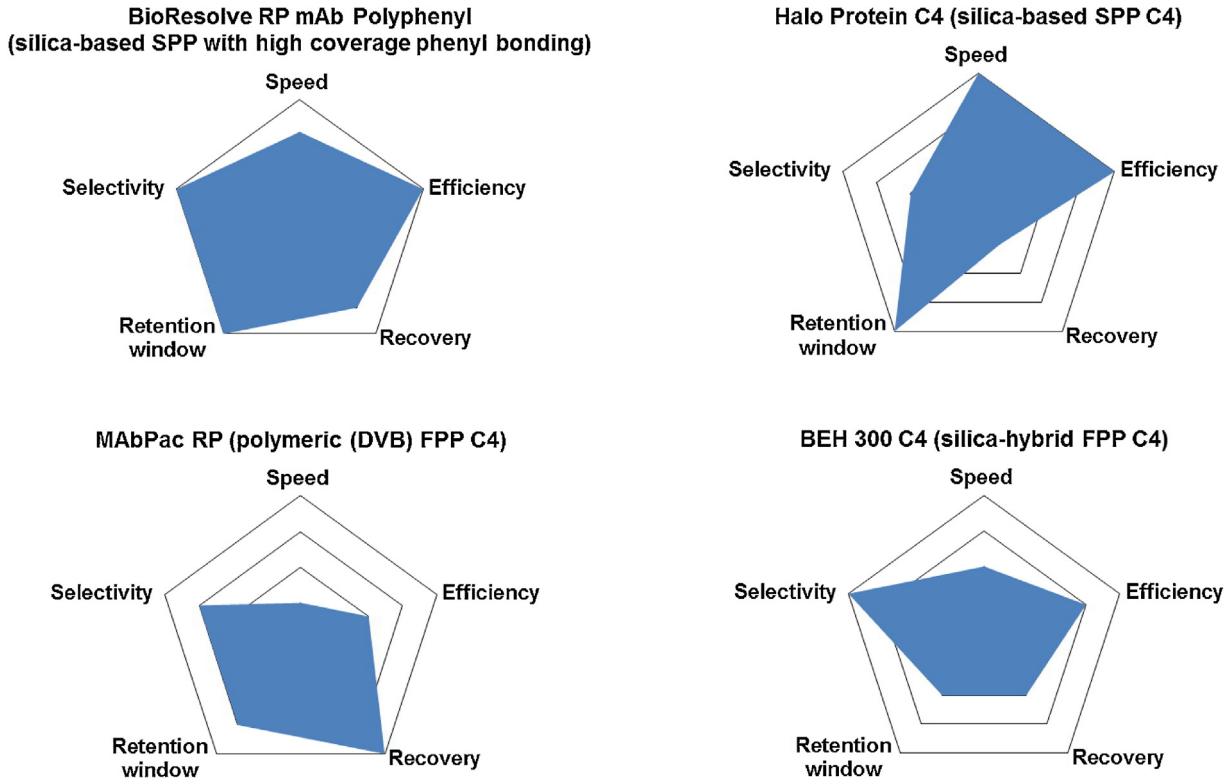

Fig. 8. Spidergram representation of the features of the different wide-pore columns based on selectivity, retention window, recovery, efficiency (peak capacity) and separation speed (permeability × operating pressure capability).

chain (H0). The second objective in the RPLC analysis of a cysteine linked ADC is to separate – if possible – the variants related to the light- and heavy chain, such as post-translational modifications and positional DAR isomers. As can be seen on Fig. 6B, the most favorable selectivity between the L1 and H0 peaks was again observed with the BioResolve column. The MAbPac RP column also provided a good separation between these critical peaks. Meanwhile, the other three columns produced selectivity between these peaks that was significantly lower and in one case notably inadequate (HALO Protein C4). The following resolutions were achieved between the L1 and H0 peaks; $Rs = 11.30$ (BioResolve RP mAb Polyphenyl), 5.14 (MAbPac RP), 2.88 (BEH 300 C4), 2.19 (Aeris WP C18) and 1.35 (HALO Protein C4). The largest number of variants separated from the main peaks was also obtained on the BioResolve column (see the shoulder peaks of H0, H2 and H3). These results confirm that the additional selectivity afforded by a high coverage phenyl bonded phase (as related to steric and/or π-π interactions) is important to discriminate protein species.

3.4. The impact of mobile phase additives

Studies were also performed to investigate the effect of replacing some of the TFA ion pairing additive of the mobile phase with FA. Elution profiles of the reduced brentuximab vedotin and reduced, IdeS digested NIST mAb were studied on the BioResolve column and on a reference silica based column, namely the HALO Protein C4. For the reduced brentuximab vedotin, the elution profile of loaded and unconjugated ADC fragments slightly changed when TFA was gradually replaced by FA (Fig. 7A and B). Retention and resolution of the pre- and post-peaks of the major species decreased on both columns when replacing TFA with FA. Moreover, recovery of the most critical, highly hydrophobic H3 fragment, decreased to 72% on the HALO and to 79% on the BioResolve material when using 0.01% TFA + 0.09% FA in the mobile phase. The average peak capacity of the six major peaks decreased by 42% on the HALO and 23% on the BioResolve column. From this example, 0.1% TFA can be replaced by 0.05% TFA/0.05% FA without serious peak distortion and any significant loss of efficiency on both columns, and above all on the BioResolve column. Further decreases in TFA may result in severe peak tailing and compromised resolution but it is sample dependent. Similar behavior was observed for the NIST mAb fragments (Fig. 7C and D). Indeed, selectivity changed only slightly when using 0.05% TFA + 0.05% FA, while resolution and recovery of the major peaks were maintained. Interestingly, the area of the Fd' pre-peak – which may correspond to an artifactual internal cleavage between D_{88}-P_{89} [50,51] – is markedly reduced at low TFA concentrations compared to other peaks. It is reasonable to suggest that this putative degradation artifact is catalyzed by strongly acidic conditions, explaining why its abundance is quite high with 0.1% TFA (pH values for 0.1% TFA and 0.01% TFA + 0.09% FA are ~2.0 and 2.5, respectively). This is corroborated by the fact that the area of this peak increased significantly when longer gradient times and higher temperatures were explored to optimize selectivity. This result also demonstrates that it may be pragmatic to reduce TFA concentrations whenever possible simply to limit the formation of degradation products. Moreover, partial replacement of TFA with FA is expected to increase MS sensitivity. The possibilities and limitations of the BioResolve column for use with MS detection will be systematically evaluated in a forthcoming study.

3.5. Overall comparison of the columns

Numerous parameters should be considered to select the best column for a given purpose, including selectivity, retentivity, efficiency, separation speed and recovery (adsorption). To select the most appropriate column, all of these figures of merits have been combined in the spidergrams of Fig. 8 for four modern wide-pore RPLC columns (silica-based SPP with a high coverage phenyl bond-

ing, silica-based SPP C4, polymeric (DVB) FPP and silica-hybrid FPP C4). Selectivity was ranked on the basis of average selectivity for NIST mAb and ADC samples under optimal conditions. Retention windows were determined for both samples based on the difference between the retention of the last and the first eluting peaks ($k_{app,last}$–$k_{app,first}$) under generic conditions. Recovery was considered for the worst case sample (intact panitumumab). Finally, efficiency was compared based on the achievable peak capacity while separation speed was assessed according to column permeability and maximum operating pressure.

If all these features are considered, it appears that the best balance of performance is provided by the BioResolve column. If only the efficiency and separation speed are taken into account, then the silica-based HALO C4 protein is also a good choice. In contrast, if the recovery is the most important parameter (e.g. determination of average DAR) – and efficiency and separation speed are not an issue – then one of the best options is a polymer based FPP material (like that of the mAb Pac RP column).

4. Conclusion

A new stationary phase based on a high coverage phenyl bonding and a wide-pore silica-based SPP has been characterized and compared to other recently developed wide-pore RPLC phases. With this cohort of column technologies, it has been possible to observe the effects of differences in stationary phase morphology, composition and surface chemistry on the analysis of various mAbs and a cysteine linked IgG1 type ADC.

This new SPP material is based on 2.7 μm particles with *rho* = 0.70 (corresponding to 0.40 μm shell thickness) and its average pore size is ∼450 Å. Its total porosity is ε_T = 0.65 and it has a permeability of $K_v = 1.4 \times 10^{-10}$ cm^2.

The achievable peak capacity for intact mAb and sub-units was somewhat higher (or equivalent in some cases) to the peak capacity achievable with one of the most efficient wide-pore SPP columns that is currently commercially available (the HALO Protein C4 column). Peak capacity values between n_c = 100 and 175 were observed for intact NIST mAb with a 150 × 2.1 mm column, when the gradient time was set between 5 and 40 min.

In terms of protein recovery, the new stationary phase was seen to be superior to silica-based and silica-hybrid materials bonded with C4 ligands. It shows only slightly lower, almost negligible, recovery differences compared to a DVB polymer-based material. For most mAbs, it appears that acceptable recoveries might be achieved even at 70 °C versus the 80 or 90° C temperatures now being routinely used.

Due to its unique surface chemistry, this new phase exhibits novel selectivity for mAb sub-unit peaks and ADC DAR species as compared to commonly used C4 or C18 ligands. Minor peaks representing variants could be successfully separated between the Fc/2 and LC sub-units of NIST mAb, something not possible with the other stationary phases included in this study. Further work is planned to identify these variants of NIST mAb.

Attempts were made to decrease concentration of TFA ion pairing agent to facilitate improved MS sensitivity. Through which, it was found that TFA concentration can be decreased without significant loss in recovery or peak capacity with this new column. In addition, it was shown that replacing TFA with FA can also be beneficial to avoid the formation of undesired degradation products (such as the artifactual internal cleavage between D_{88}-P_{89} amino acids of NIST mAb).

When considering all the important parameters of mAb or ADC separations (selectivity, retention window, peak capacity, separation speed and recovery), this new column technology, based on a uniquely high coverage phenyl bonding and wide-pore silica based SPP material seems to be most promising. In many ways, it appears that this column advantageously marries the kinetic properties of a modern superficially porous particle with the desirable chemical properties of a polymeric divinyl benzene based stationary phase.

Acknowledgement

Davy Guillarme wishes to thank the Swiss National Science Foundation for support through a fellowship to Szabolcs Fekete (31003A159494).

References

[1] W. Chen, K. Jiang, A. Mack, B. Sachok, X. Zhu, W.E. Barber, X. Wang, Synthesis and optimization of wide pore superficially porous particles by a one-step coating process for separation of proteins and monoclonal antibodies, J. Chromatogr. A 1414 (2015) 147–157.
[2] C. Horváth, S.R.J. Lipsky, Rapid analysis of ribonucleosides and bases at the picomole level using pellicular cation exchange resin in narrow bore columns, Anal. Chem. 41 (1969) 1227–1234.
[3] J.J. Kirkland, Controlled surface porosity supports for high-speed gas and liquid chromatography, Anal. Chem. 41 (1969) 218–220.
[4] J.J. Kirkland, P.C. Yates, U.S. Patent 3, 3722,181, March 27, 1973.
[5] J.J. Kirkland, High speed liquid-partition chromatography with chemically bonded organic stationary phases, Chromatogr. Sci. 9 (1971) 206–214.
[6] J.J. Kirkland, Porous silica microsphere column packings for high-speed liquid – liquid chromatography, J. Chromatogr. A 83 (1973) 149–167.
[7] J.J. Kirkland, Superficially porous silica microspheres for the fast high-performance liquid chromatography of macromolecules, Anal. Chem. 64 (1992) 1239–1245.
[8] J.J. Kirkland, F.A. Truszkowski, C.H. Dilks Jr., G.S. Engel, Superficially porous silica microspheres for fast high-performance liquid chromatography of macromolecules, J. Chromatogr. A 890 (2000) 3–13.
[9] S. Fekete, E. Oláh, J. Fekete, Fast liquid chromatography: the domination of core–shell and very fine particles, J. Chromatogr. A 1228 (2012) 57–71.
[10] S. Fekete, J. Schappler, J.L. Veuthey, D. Guillarme, Current and future trends in UHPLC, Trends Anal. Chem. 63 (2014) 2–13.
[11] G. Guiochon, F. Gritti, Shell particles trials tribulations triumphs, J. Chromatogr. A 1218 (2011) 1915–1938.
[12] S. Fekete, J.L. Veuthey, D. Guillarme, New trends in reversed-phase liquid chromatographic separations of therapeutic peptides and proteins: theory and applications, J. Pharm. Biomed. Anal. 69 (2012) 9–27.
[13] F. Gritti, G. Guiochon, The mass transfer kinetics in columns packed with HALO-ES shell particles, J. Chromatogr. A 1218 (2011) 907–921.
[14] S.A. Schuster, B.M. Wagner, B.E. Boyes, J.J. Kirkland, Wider pore superficially porous particles for peptide separations by HPLC, J. Chromatogr. Sci. 48 (2010) 566–571.
[15] S.A. Schuster, B.E. Boyes, B.M. Wagner, J.J. Kirkland, Fast high performance liquid chromatography separations for proteomic applications using Fused-Core® silica particles, J. Chromatogr. A 1228 (2012) 232–241.
[16] S. Fekete, R. Berky, J. Fekete, J.L. Veuthey, D. Guillarme, Evaluation of a new wide pore core–shell material (Aeris™ WIDEPORE) and comparison with other existing stationary phases for the analysis of intact proteins, J. Chromatogr. A 1236 (2012) 177–188.
[17] S. Fekete, R. Berky, J. Fekete, J.L. Veuthey, D. Guillarme, Evaluation of recent very efficient wide-pore stationary phases for the reversed-phase separation of proteins, J. Chromatogr. A 1252 (2012) 90–103.
[18] S.A. Schuster, B.M. Wagner, B.E. Boyes, J.J. Kirkland, Optimized superficially porous particles for protein separations, J. Chromatogr. A 1315 (2013) 118–126.
[19] B.M. Wagner, S.A. Schuster, B.E. Boyes, T.J. Shields, W.L. Miles, M.J. Haynes, R.E. Moran, J.J. Kirkland, M.R. Schure, Superficially porous particles with 1000 Å pores for large biomolecule high performance liquid chromatography and polymer size exclusion chromatography, J. Chromatogr. A 1489 (2017) 75–85.
[20] A. Ahmed, W. Abdelmagid, H. Ritchie, P. Myers, H. Zhankg, Investigation on synthesis of spheres-on-sphere silica particles and their assessment for high performance liquid chromatography applications, J. Chromatogr. A 1270 (2012) 194–203.
[21] S. Fekete, M. Rodriguez-Aller, A. Cusumano, R. Hayes, H. Zhang, T. Edge, J.L. Veuthey, D. Guillarme, Prototype sphere-on-sphere silica particles for the separation of large biomolecules, J. Chromatogr. A 1431 (2016) 94–102.
[22] S. Fekete, S. Rudaz, J.L. Veuthey, D. Guillarme, Impact of mobile phase temperature on recovery and stability of monoclonal antibodies using recent reversed-phase stationary phases, J. Sep. Sci. 35 (2012) 3113–3123.
[23] S. Fekete, A. Beck, E. Wagner, K. Vuignier, D. Guillarme, Adsorption and recovery issues of recombinant monoclonal antibodies in reversed-phase liquid chromatography, J. Sep. Sci. 38 (2015) 1–8.
[24] D.S. Rehder, T.M. Dillon, G.D. Pipes, P.V. Bondarenko, Reversed-phase liquid chromatography/mass spectrometry analysis of reduced monoclonal antibodies in pharmaceutics, J. Chromatogr. A 1102 (2006) 164–175.
[25] D. Ren, G. Pipes, G. Xiao, G.R. Kleemann, P.V. Bondarenko, M.J. Treuheit, H.S. Gadgil, Reversed-phase liquid chromatography–mass spectrometry of

site-specific chemical modifications in intact immunoglobulin molecules and their fragments, J. Chromatogr. A 1179 (2008) 198–204.
[26] B. Bobaly, V. D'Atri, A. Goyon, O. Colas, A. Beck, S. Fekete, D. Guillarme, Protocols for the analytical characterization of therapeutic monoclonal antibodies. II – Enzymatic and chemical sample preparation, J. Chromatogr. B 1060 (2017) 325–335.
[27] J. Sjörgen, F. Olsson, A. Beck, Rapid and improved characterization of therapeutic antibodies and antibody related products using IdeS digestion and sub-unit analysis, Analyst 141 (2016) 3114–3125.
[28] J.C. Giddings, Maximum number of components resolvable by gel filtration and other elution chromatographic methods, Anal. Chem. 39 (1967) 1027–1028.
[29] C. Horváth, S.R.J. Lipsky, Peak capacity in chromatography, Anal. Chem. 39 (1967) 1893.
[30] U.D. Neue, Theory of peak capacity in gradient elution, J. Chromatogr A 1079 (2005) 153–161.
[31] X. Wang, D.R. Stoll, A.P. Schellinger, P.W. Carr, Peak capacity optimization of peptide separations in reversed-phase gradient elution chromatography: fixed column format, Anal. Chem. 78 (2006) 3406–3416.
[32] J.W. Dolan, L.R. Snyder, N.M. Djordjevic, D.W. Hill, T.J. Waeghe, Reversed-phase liquid chromatographic separation of complex samples by optimizing temperature and gradient time: i. Peak capacity limitations, J. Chromatogr. A 857 (1999) 1–20.
[33] U.D. Neue, J.R. Mazzeo, A theoretical study of the optimization of gradients at elevated temperature, J. Sep. Sci. 24 (2001) 921–929.
[34] U.D. Neue, J.L. Carmody, Y.F. Cheng, Z. Lu, C.H. Phoebe, T.E. Wheat, Design of rapid gradient methods for the analysis of combinatorial chemistry libraries and the preparation of pure compounds, Adv. Chromatogr. 41 (2001) 93–136.
[35] L.R. Snyder, in: C. Horvath (Ed.), Gradient Elution in HPLC: Advances and Perspectives, Vol. 1, Academic Press, New York, 1980.
[36] L.R. Snyder, J.J. Kirkland, J.L. Glajch, Practical HPLC Method Development, second ed., John Wiley & Sons Inc., New York, 1997.
[37] P.A. Bristow, J.H. Knox, Standardization of test conditions for high performance liquid chromatography columns, Chromatographia 10 (1977) 279–289.
[38] S. Fekete, J. Fekete, Fast gradient screening of pharmaceuticals with 5 cm long, narrow bore reversed-phase columns packed with sub-3 μm core–shell and sub-2 μm totally porous particles, Talanta 84 (2011) 416–423.
[39] X. Wang, W.E. Barber, P.W. Carr, A practical approach to maximizing peak capacity by using long columns packed with pellicular stationary phases for proteomic research, J Chromatogr. A 1107 (2006) 139–151.
[40] S. Fekete, I. Molnar, D. Guillarme, Separation of antibody drug conjugate species by RPLC: A generic method development approach, J. Pharm. Biomed. Anal. 137 (2017) 60–69.
[41] A.B. Scholten, H.A. Claessens, J.W. de Haan, C.A. Cramers, Chromatographic activity of residual silanols of alkylsilane derivatized silica surfaces, J. Chromatogr. A 759 (1997) 37–46.
[42] S. Kayillo, G.R. Dennis, R.A. Shalliker, An assessment of the retention behaviour of polycyclic aromatic hydrocarbons on reversed phase stationary phases: selectivity and retention on C18 and phenyl-type surfaces, J. Chromatogr. A 1126 (2006) 283–297.
[43] S. Kayillo, G.R. Dennis, R.A. Shalliker, An assessment of the retention behaviour of polycyclic aromatic hydrocarbons on reversed phase stationary phases – thermodynamic behaviour on C18 and phenyl-type surfaces, J. Chromatogr. A 1145 (2007) 133–140.
[44] S. Kayillo, G. Dennis, R.A. Shalliker, Retention of polycyclic aromatic hydrocarbons on propyl-phenyl stationary phases in reversed-phase high performance liquid chromatography, J. Chromatogr. A 1148 (2007) 168–176.
[45] C.M. Vera, D. Shock, G.R. Dennis, J. Samuelsson, M. Enmark, T. Fornstedt, R.A. Shalliker, Contrasting selectivity between HPLC and SFC using phenyl-type stationary phases: a study on linear polynuclear aromatic hydrocarbons, Microchem. J. 119 (2015) 40–43.
[46] K. Jinno, T. Nagoshi, N. Tanaka, J.C. Fetzer, W.R. Biggs, Eluation behaviour of planar and non-planar polycyclic aromatic hydrocarbons on various chemically bonded stationary phases in liquid chromatography, J. Chromatogr. A 392 (1987) 75–82.
[47] Y. Chen, C.T. Mant, R.S. Hodges, Temperature selectivity effects in reversed-phase liquid chromatography due to conformation differences between helical and non-helical peptides, J. Chromatogr. A 1010 (2003) 45–61.
[48] C.T. Mant, Y. Chen, R.S. Hodges, Temperature profiling of polypeptides in reversed-phase liquid chromatography: I. Monitoring of dimerization and unfolding of amphipathic α-helical peptides, J. Chromatogr. A 1009 (2003) 29–43.
[49] C.T. Mant, B. Tripet, R.S. Hodges, Temperature profiling of polypeptides in reversed-phase liquid chromatography: II. Monitoring of folding and stability of two-stranded α-helical coiled-coils, J. Chromatogr. A 1009 (2003) 45–59.
[50] V. Faid, Y. Leblanc, N. Bihoreau, G. Chevreux, Middle-up analysis of monoclonal antibodies after combined IgdE and IdeS hinge proteolysis: investigation of free sulfhydryls, J. Pharm. Biomed. Anal. 149 (2018) 541–546.
[51] J.E. Schiel, D.L. Davis, O.V. Borisov, State-of-the-Art and Emerging Technologies for Therapeutic Monoclonal Antibody Characterization Volume 2 Biopharmaceutical Characterization: The NISTmAb Case Study, 2015.